www.czasopisma.pan.pl PAN POLSKA AKADEMIA NAUK www.journals.pan.pl

Arch. Min. Sci. **68** (2023), 2, 351-370

Electronic version (in color) of this paper is available: http://mining.archives.pl

DOI: https://doi.org/10.24425/ams.2023.146184

DAQIANG XU[1,2], PEISEN ZHANG[1,2*], WEI YAN[1,2], XIAOLE ZHANG[1,2], YUHANG DONG[1,2], HUI NIU[1,2]

MECHANICAL PROPERTIES AND ENERGY OF SANDSTONE UNDER CYCLIC LOADING IN EVOLUTIONARY PATTERN EXPERIMENTAL STUDIES

In order to explore the mining failure law of deep coal seam floor and clarify the mechanical behavior and energy change in the floor strata during mining, the mechanical properties and energy evolution law of sandstone under cyclic loading with different confining pressures (20, 30, 40 MPa) were studied using the Rock Top multi-field coupling tester. The results are as follows: (1) the hysteresis phenomenon of a rock stress-strain curve under cyclic loading is evident. Moreover, the hysteresis loop migrates to the direction of strain increase, and the fatigue damage caused by cyclic loading has a certain weakening effect on the peak strength of rock; (2) both the number of cycles and the axial strain show a nonlinear change characteristic that satisfies the quadratic function relationship. Among them, the stress level of the rock is the main factor affecting the fitting effect; (3) under the same confining pressure, with an increase in cycle level, the macroscopic deformation of the rock increases, the accumulation of fatigue damage in the sample increases, and the irreversible deformation of the rock increases, which leads to an increase in energy input and dissipation; (4) in terms of elastic energy and dissipation energy, elastic energy plays a dominant role. In the initial cycle, the rock is destroyed, and the rock energy loss is great. After the second cycle, the input energy is mainly stored in the rock in the form of elastic energy, and only a small part of the input energy is released in the form of dissipation energy; (5) the confining pressure can improve the efficiency of rock absorption and energy storage, enhance the energy storage limit of rock, and limit the dissipation and release of partial energy of rock. The greater the confining pressure, the more evident the limiting effect, and the more significant the dominant position of elastic energy; and (6) the change in the energy dissipation ratio can be divided into three stages: rapid decline stage, stable development stage and rapid rise stage. The greater the increase in dissipation energy, the greater the degree of rock damage. The evolution process of the energy dissipation ratio can reflect the internal damage accumulation process of rock well, which can be used as the criterion of rock instability.

Keywords: rock mechanics; cyclic loading; mechanical property; energy evolution; instability criterion

[1] SHANDONG UNIVERSITY OF SCIENCE AND TECHNOLOGY, NATIONAL KEY LABORATORY FOR MINE DISASTER PREVENTION AND CONTROL, QINGDAO, SHANDONG 266590, CHINA

[2] SHANDONG UNIVERSITY OF SCIENCE AND TECHNOLOGY, NATIONAL DEMONSTRATION CENTER FOR EXPERIMENTAL MINING ENGINEERING EDUCATION, QINGDAO, SHANDONG 266590, CHINA

* Corresponding author: sdkjd_304a@126.com

1. Introduction

With the continuous increase in resource demand and mining intensity, shallow resources are depleting. Hence, it has become an inevitable trend for resource mining to deepen. However, deep mining faces a complex geological environment with 'three highs and one disturbance' (high ground stress, high earth temperature, high osmotic pressure, and engineering disturbance, respectively), causing vastly different mechanical behaviours of rocks from those in shallow mining [1-5]. A direct consequence of this difference is the increase in mining problems associated with rock pressure [6]. For deep underground projects, the stresses on rocks are frequently changing dynamic loads, i.e., cyclic loads [7-8], whose mechanical behaviour and energy variations are more complex than those under conventional loading. Therefore, the study of the mechanical properties and energy evolution of a rock mass under cyclic loading can offer insight into the deformation and failure characteristics of an underground rock mass, which is of great significance to the design and operation of underground engineering performed under complex geological environment, such as mining engineering.

The rock deformation and failure process is accompanied with the input, accumulation, dissipation, and release of energy, which are repeatedly experienced by rocks under cyclic loading. From a mechanical viewpoint, the above process is from local rupture to partial damage to overall instability. From a thermodynamic perspective, the rock deformation and failure process is a process of energy dissipation and release, whereas rock instability failure is a result of the instantaneous release of energy in rocks [9-10]. The instability process of rock can be quantitatively characterized by relevant rock mechanical parameters, which are usually obtained directly from boreholes. However, this geotechnical test procedure is time-consuming and costly [11]. It is relatively simple to determine the relevant mechanical properties of rock through laboratory tests [12-13]. Dvornikov et al. [14] provided the criteria for determining the strength properties of rock suitable for mining engineering tasks and introduced the rock failure energy strength estimation test bench. Thus far, many experimental studies have been conducted on the mechanical properties and energy evolution of different types of rocks under cyclic loading. For instance, uniaxial cyclic loading tests on sandstone specimens have found that the peak strength of the rocks decreases under cyclic loading. Moreover, the modulus of elasticity in the unloading stage is typically larger than that in the loading stage, whereas the overall modulus of elasticity first increases and subsequently decreases with increasing upper cyclic loading [15-17]. During cyclic loading, the stress-strain curve show a remarkable hysteresis, suggesting an apparent residual strain. Rock damage gradually accumulates and develops in three stages: decelerated, stable, and accelerated accumulation [18-20]. In addition, Hong et al. [21] conducted uniaxial cyclic loading and unloading tests on dry and saturated sandstone samples, and found that the average peak strength, elastic modulus, elastic energy, and dissipation energy of saturated samples are lower than those of dry samples. Ying et al. [22] conducted uniaxial cyclic loading tests on mudstone, and determined that the proportion of the initial cyclic energy dissipation rapidly increases when the sample enters the elastic section and abruptly increases when it approaches failure. Jin et al. [23] conducted uniaxial cyclic loading tests on marble, and revealed that the initial stress level is the main factor for its failure of marble, and the amplitude is secondary. Uniaxial cyclic loading tests on coal rocks have shown that their compressive strength decreases under cyclic loading [24] and that the modulus of elasticity increases with increasing number of cycles and eventually decreases with the increase in the upper stress. The number of cycles and the elastic strain energy are positively correlated with the hysteresis loop area [25-26]. Srinivasan et al. [27]

divided rock samples into different degrees of rock stress memory according to the characteristics that rock can retain stress after loading. The higher damage caused by the initial loading and rock fracture is the reason for the poor stress memory of rock. It can be seen that the mechanical properties of rock under cyclic loading are different from those under conventional loading. The stress level of rock is the main reason for the difference in the rock properties. The damage evolution of rock is mainly controlled by initial loading and failure stress. Therefore, according to different engineering conditions, based on different stress levels, the mechanical properties of rock will be different. In studies, conventional triaxial and cyclic loading tests have been conducted on different types of rocks such as sandstone, granite, and coal rocks. Triaxial cyclic load tests on sandstone have shown that the cyclic load action increases rock failure and that the energy dissipation ratio can reflect the evolution of internal failure and plastic deformation of a rock to a certain extent [28]. Moreover, the stress-axial strain curve has been found to be concave and shift in the direction of increasing strain [29]. The peak strength of a rock is relatively lower in triaxial cyclic load tests than that in conventional triaxial tests [30], whereas the axial peak strain is higher in the former. Increasing the confining pressure can improve the resistance of a rock to deformation. With the increase in the upper limit stress, the area of the hysteresis loop gradually increases, and consequently, the dissipation energy gradually accumulates. The hysteresis loop area is negatively correlated with the change om the confining pressure, whereas positively correlated with the change in the axial load [31-32]. Yuan et al. [33] fitted the hysteresis loop loading and unloading sections of sandstone with a quadratic fit separately. However, there is little research on post-peak energy characteristics. Therefore, Qingbin et al. [34] conducted triaxial cyclic loading tests on tuffs with different confining pressures to reveal the pre- and post-peak energy evolution and distribution patterns of the confining pressure of loaded rock samples. Shishu et al. [35] conducted an experimental study on the damage characteristics of sandstone under cyclic loading with different frequencies. It showed that a high loading frequency implies a large residual axial strain at the time of damage, considerable damage, and high initial stiffness of a rock sample. Ruidong et al. [36] conducted triaxial cyclic loading tests on coal rocks, and found that their dissipation energies increase with the increase in the upper limit stress. Peng et al. [37] performed numerical simulations of real triaxial cyclic loading on rock assemblages using the RFPA^{3D} parallel calculation program. They found that the local damage was considerable and the damage location was related to soft and hard rocks. Triaxial cyclic load tests on granite have found that granite samples under different confining pressures present remarkable characteristics of brittle damage, with macroscopic failure being mainly shear damage. The peak strength and damage stress of a sample increased with increasing confining pressure; the dissipation energy was significantly correlated with the confining pressure and the number of loading cycles [38-39]. It can be seen that confining pressure and axial load determine the mechanical properties and energy evolution of rock. The rock energy theory and its application are very important for analyzing the essential causes of rock failure and optimizing rock engineering design and construction. Overall, relatively comprehensive studies on energy characteristics and distribution in terms of the characteristic stresses and unique stages for different types of rocks have been conducted. These have considerable potential in the development of a rock energy theory and practical engineering applications.

The above research results provide important guidelines to successfully conduct experimental research on the mechanical properties and energy evolution law of sandstone under cyclic loading in this study. However, the lower limit stress of cyclic loading in the above studies was generally taken as 0 MPa or kept at the same level. Moreover, the unloading amount was only controlled

by changing the upper limit stress. However, the rock engineering approach is established for situations encountered in civil engineering and mining engineering [40]. For example, in mining engineering, with the advance of the working face, along with the hydraulic support cycle, the falling-moving-lifting operation is conducted, resulting in alternating changes in unloading and loading of the floor, and the vertical stress of the floor rock mass is affected by the superposition of the support. The degree of influence will eventually show a 'no-weak-strong-weak' change [41]. In contrast, in actual engineering, the lower limit stress is not unloaded to 0 MPa or stabilized at a certain stress level when the rock mass is disturbed by engineering. Instead, the upper and lower limit stresses may increase. Therefore, in this study, using a rock top multi-field coupling tester, a synchronous but unequal increase in the upper and lower limit stresses was achieved by loading the axial stress difference in equal gradient and unloading the maximum stress of the rock sample in the same state and percentage. An experimental study on the mechanical properties and energy evolution law of sandstone under cyclic loading was conducted using different loading and unloading methods, and it can serve as a reference for geotechnical engineering safety problems in complex geological environment such as mining engineering.

2. Experimental overview

Sandstone is a sedimentary rock extensively distributed in the crust of the earth, and it is a common rock type in the field of underground engineering. The sandstone used for the tests was cored from the adjacent part of the intact rock mass with an even texture and no remarkable joints and fissures. Subsequently, it was polished to realize a uniform and fine appearance with flat ends. Samples were prepared according to the standard in [42], with dimensions of ϕ50 mm × H100 mm and allowable deviations of ±0.03 mm in the end flatness and ±0.25°. However, rock masses are naturally heterogeneous, and two rock samples with the same volume characteristics may also exhibit great differences in microstructure [43]. In order to eliminate the influence of sandstone discreteness on the test results as much as possible, the vacuum pumping method was used before the test. The sandstone sample was subjected to a 6 h forced saturation treatment; then, an acoustic wave test that was performed using JSR-DPR 300 ultrasonic equipment. The sandstone sample with the abnormal wave velocity was discarded, and the sandstone sample with small difference was selected for the test to meet the test requirements.

The instrument used in these tests is a rock top multi-field coupling tester, as shown in Fig. 1. The instrument consists of a control system, an axial pressure system, a confining pressure system, a triaxial pressure chamber, and specialized high-precision sensors (displacement and pressure). The axial and confining pressure systems can apply maximum 500 MPa axial pressure and 60 MPa confining pressure. The triaxial pressure chamber is equipped with an LVDT axial displacement sensor and circumferential strain gauge, and the triaxial pressure outdoor is not equipped with sensor. The LVDT displacement sensor which is used to record the axial deformation of rock and calculate the axial strain has a range of 12 mm and an accuracy of ±0.001 mm. The circumferential strain gauge can obtain the lateral strain of rock by recording voltage changes. In addition, it can record stress differences, confining pressure, and other data simultaneously. The above recorded data are used in this study.

The sandstone samples were divided into two groups, group C and group X. Those in group C were subjected to conventional triaxial tests, while those in group X were subjected to cyclic loading tests. The labels C20, X20-1, X20-2 and X30-1 are different rock samples, and each

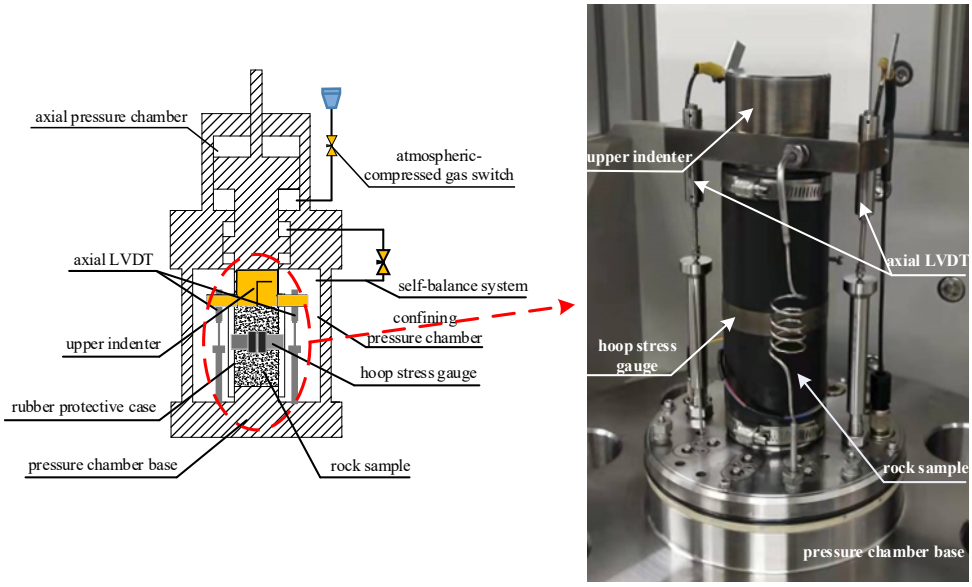

Fig. 1. Rock top multi-field coupled tester

rock sample was labelled. Three parallel tests were carried out. Among them, the conventional triaxial test group was primarily used for comparative analysis. The rock sample numbers and the test parameters are listed in Table 1.

TABLE 1

Rock sample numbers and test parameters

Confining Pressure	Sample Number	Loading Method	Cycle rank	Unloading Capacity
20	C20	Conventional triaxial loading	Three-stage cycle	0
	X20-1	cyclic loading	Three-stage cycle	25%
	X20-2	cyclic loading	Three-stage cycle	50%
	X20-3	cyclic loading	Three-stage cycle	75%
30	C30	Conventional triaxial loading	Four-stage cycle	0
	X30-1	cyclic loading	Four-stage cycle	25%
	X30-2	cyclic loading	Four-stage cycle	50%
	X30-3	cyclic loading	Four-stage cycle	75%
40	C40	Conventional triaxial loading	Four-stage cycle	0
	X40-1	cyclic loading	Four-stage cycle	25%
	X40-2	cyclic loading	Four-stage cycle	50%
	X40-3	cyclic loading	Four-stage cycle	75%

The specific test steps were as follows:

(1) The rock samples were encapsulated in a triaxial pressure chamber, and installations such as the transducer and the strain gauge were inspected.
(2) A self-balance device was turned on, and a hydrostatic pressure was applied at a rate of 1 MPa/min in a stress-controlled manner to $\sigma_1 = \sigma_2 = \sigma_3$, and the predetermined values of the initial hydrostatic pressure were 20, 30, and 40 MPa.
(3) An axial pressure was loaded according to different schemes.

In the 20 MPa perimeter pressure test group, the C20 sample was directly loaded at a constant rate of 0.02 mm/min in the displacement control mode until the sample was damaged. The X20-1 sample was loaded at a constant rate of 0.02 mm/min in the displacement control mode with a stress difference of 40 MPa in equal gradients (each increase of 40 MPa for cyclic load testing was considered as an additional cycle). Then, the stress difference of 25% (e.g., 40 MPa → 30 MPa) was removed at a constant rate of 1 MPa/min in the stress control mode, and the cycle was repeated three times, and then the cycle level was increased until the rock sample was destroyed. X20-2 and X20-3 were unloaded by 50% (e.g., 40 MPa → 20 MPa) and 75 % (e.g., 40 MPa 10 MPa), respectively, and the remaining operations were consistent.

Change the initial hydrostatic pressure predetermined value (30, 40 MPa), repeat the above steps to complete the test.

3. Experimental Results and Analysis

3.1. Analysis of Rock Mechanical Properties Under Cyclic Loading

The stress-strain curves of the rock samples under different cyclic loads are shown in Fig. 2 (taking the confining pressure of 20 MPa as an example). Noticeably, the stress-axial/lateral/volumetric strain curves under cyclic loads show remarkable hysteresis, and the hysteresis loop gradually shifts in the direction of strain increase. This is caused by the inconsistency in the paths of compression and tension between particles during loading and unloading [44], as the rock matrix is always alternating between compression and expansion under cyclic loading. Moreover, the particles inside the skeleton move along the centre line of the particles in reciprocation

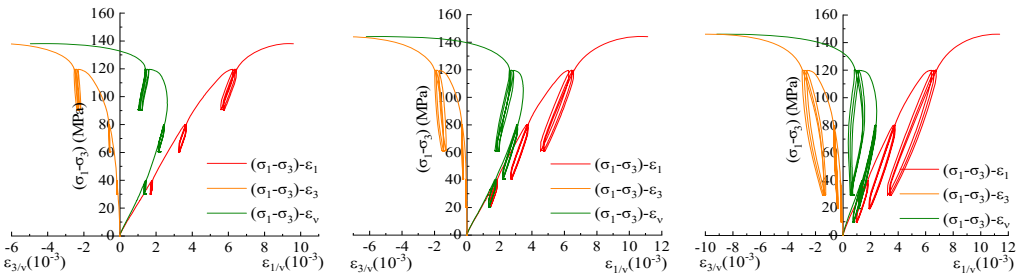

Fig. 2. Stress-strain curves under 20 MPa confining cyclic load

in the axial and lateral directions. The unloading curve does not return along the original path; therefore, the loading and unloading curves do not overlap. This phenomenon suggests that the rock is neither a completely elastic nor a plastic body but an elastic-plastic body with defects such as primary microfractures and pores. In addition, with the increase in the upper limit stress, the hysteresis loop gradually tends to be 'sparse' and the hysteresis loop area gradually enlarges. The analysis suggests that with the increase in the upper limit stress, the compression path of the internal rock matrix particles, compression amplitude, accumulation of fatigue damage inside the sample, and residual deformation of the rock increase. Consequently, the unloading curve gradually deviates from the loading curve.

The loading method and path affect the rock strength and deformation. To clarify the differences between the mechanical properties of the rock under cyclic and conventional triaxial loading under this test condition, the corresponding peak strengths and strains of the rock are compared in Figs. 3 and 4, respectively.

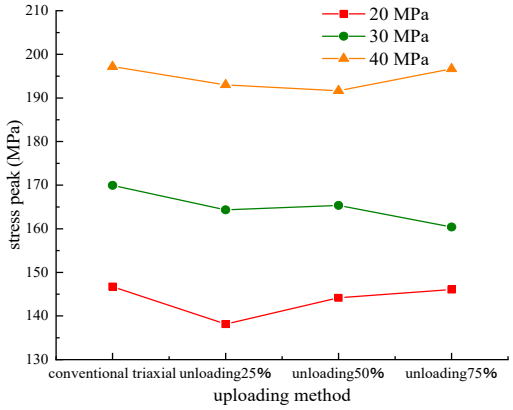

Fig. 3. Comparison of peak rock strengths

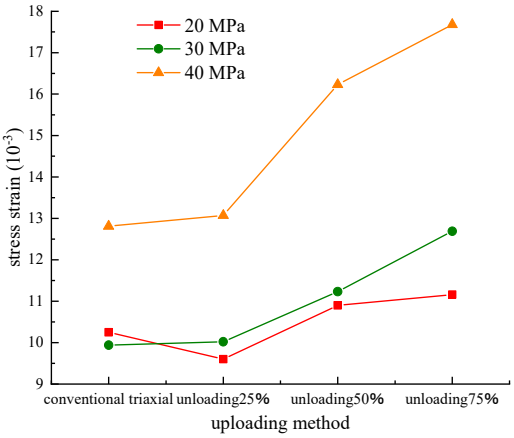

Fig. 4. Comparison of peak rock strains

As shown in Fig. 3, the peak rock strength increases with increasing confining pressure under the action of conventional triaxial and cyclic loads, indicating that the binding effect of the confining pressure can effectively improve the rock bearing capacity. The overall peak rock strengths under the cyclic loads of 20, 30, and 40 MPa confining pressure are slightly lower than those under conventional triaxial compression. This suggests that the fatigue damage caused by cyclic loads has a certain weakening effect on the peak rock strength [45]; however, the weakening effect is unremarkable.

The peak strain increases with the unloading level under the same confining pressure. The cause is that the compression–expansion amplitude of the rock matrix particles becomes larger with increasing unloading level. Consequently, the irrecoverable deformation of the rock itself gradually accumulates, which leads to the gradual increase in the peak strain of the rock. The peak strain of the rock is positively correlated with the confining pressure under the conventional triaxial and cyclic loading. In particular, the increase in the peak strain of the rock from 20 MPa to 30 MPa is small, whereas that from 30 MPa to 40 MPa is significant. This is because the rock mainly shows brittle damage characteristics between 20 and 30 MPa confining pressure, whereas its plastic characteristics increase under a high confining pressure of 40 MPa. These phenomena considerably increase the ductility of the rock, resulting in a significant increase in the peak strain.

Huafeng et al. [19] found that the stress-strain curve hysteresis phenomenon under cyclic loading is remarkable. Although Fig. 4 reflects this phenomenon to some extent, the quantitative relationship between the number of cycles and the axial strain needs to be further explored. Therefore, Fig. 5 shows the axial strain evolution patterns under different confining pressures and unloading levels

Under the confining pressure of 20 MPa, the rock experienced a three-stage cycle, compared with a four-stage cycle under the confining pressure of 30 and 40 MPa. This is attributed to the bearing capacity of the rock increasing with the confining pressure and that under the confining pressure of 20 MPa being lower than the upper stress of a four-stage cycle, as a result of which it only undergoes a three-stage cycle. From Fig. 5, both the number of cycles and axial strain show variation characteristics of a nonlinear quadratic function relationship. When the confining pressure is the same, the greater the unloading level, the smaller the lower limit stress value of the cyclic load, and the weaker the influence on the rock. Furthermore, the nonlinear fitting effect gradually tends to be optimized, and the data dispersion gradually decreases. At an unloading level of 75%, the nonlinear fitting correlation coefficient is generally greater than 0.95, and the fitting effect is better, indicating that the stress level of the rock is the main factor affecting the fitting effect. At the same unloading level, as the confining pressure increases, the fitting effect deviation becomes relatively smaller without a remarkable regularity, indicating that the influence of the confining pressure on the fitting effect is small. Under cyclic loading, the axial strain of the rock gradually increases with the increase in the number of cycles. The strain increment is larger in the first cycle than those in the other cycles, and it subsequently stabilizes regardless of the increase in the number of cycles. The above analysis suggests that in the initial cycle, the internal primary microfractures and pores are gradually compacted accompanied by interparticle misalignment friction, which increases the macroscopic deformation of the rock. After entering the second cycle, the compact rock can withstand more deformation, and its bearing capacity increases, showing a gradual deformation. When the rock is in the plastic damage stage, numerous fractures and plastic zones are produced in the initial cycle and compression

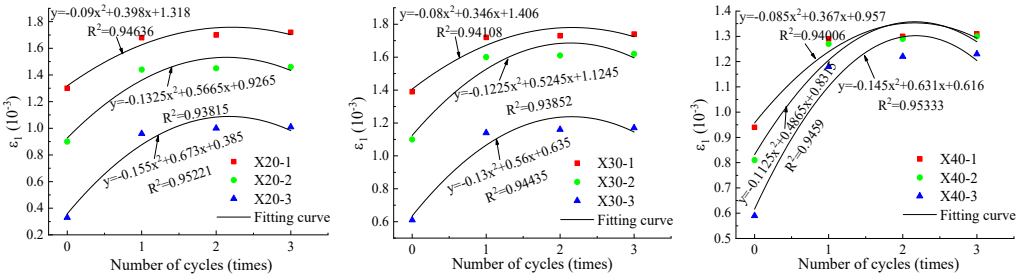

One-stage cycle

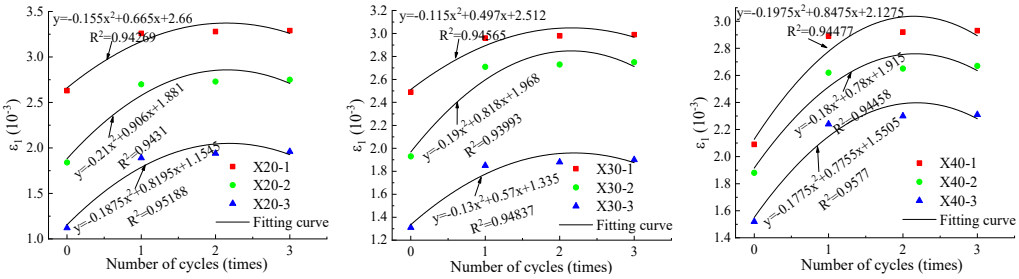

Two-stage cycle

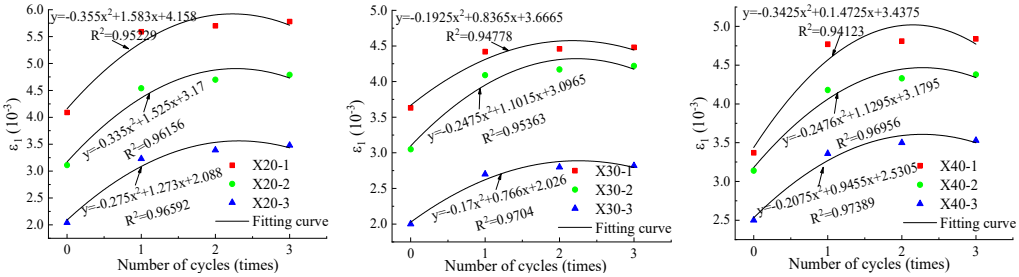

Three-stage cycle

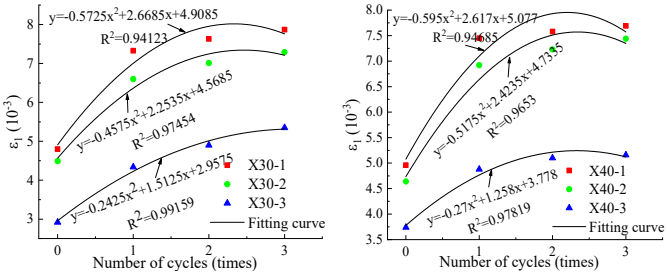

Four-stage cycle

Fig. 5. Axial strain evolution patterns under different confining pressures and unloading levels

and expansion of the existing plastic zones occur. These phenomena are accompanied by crack expansion and new crack generation after entering the second cycle, which together lead to the stabilization of the deformation tendency.

3.2. Analysis of Energy Evolution Patterns

The rock cyclic loading and unloading process is an energy input and output process, wherein the unbalanced energy input and output prevent the loading and unloading curves from overlapping, forming a hysteresis loop [46]. The hysteresis loop area can quantitatively characterize the dissipation energy [18-19,21-22]. Fig. 6 shows a schematic of the dissipation energy calculation. The input energy, U_{Si}, is the area enclosed by the first loading curve and the strain axis, and the elastic energy, U_{Ti}, is the area enclosed by the second unloading curve and the strain axis. The difference between the two energies is the dissipation energy, U_{Hi}, in the first cycle. The corresponding formula is as follows:

$$U_{Si} = \int_{\varepsilon_{Ai}}^{\varepsilon_{Bi}} \sigma_{Si} d\varepsilon \tag{1}$$

$$U_{Ti} = \int_{\varepsilon_{Bi}}^{\varepsilon_{Ci}} \sigma_{Ti} d\varepsilon \tag{2}$$

$$U_{Hi} = U_{Si} - U_{Ti} \tag{3}$$

where σ_{Si} is the i-th loading curve stress, MPa; σ_{Ti} is the i-th unloading curve stress, MPa; and ε_{Ai}, ε_{Bi}, and ε_{Ci}, correspond to the i-th loading and unloading strains at points A, B, and C, respectively.

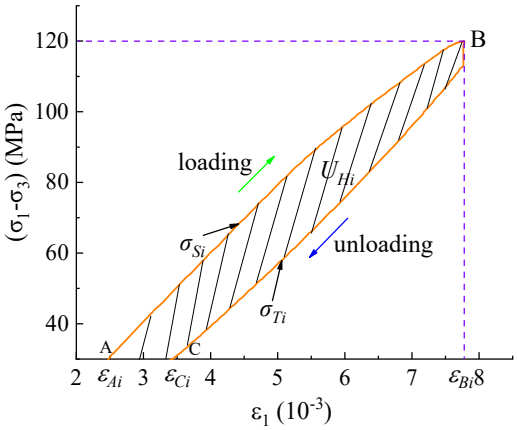

Fig. 6. Schematic of dissipation energy calculation

From the perspective of energy conservation and functional transformation, assuming that the triaxial pressure chamber is always insulated without heat transfer with the outside environment, the input energy originates from the work done on the rock by the testing machine during the triaxial compression test. Moreover, the dissipation energy is the energy lost during the loading

and unloading process when the internal micropores and fractures of the rock are compacted and squeezed and the cracks are extended as well as penetrated to form a macroscopic broken section. In addition, lateral deformation of the rock can occur under the axial load, the binding effect of the confining pressure can suppresses this lateral deformation and does negative work on it, accompanied by energy dissipation [34]. However, because the confining pressure is kept constant in these tests, the lateral deformation of the rock is continuously obstructed and the dissipation energy is low; therefore, lateral dissipation is not considered. Considering the source of the input energy, reversibility of the elastic energy, and irreversibility of the dissipation energy, the evolution patterns of the input, elastic, and dissipation energies are studied systematically. From the above analysis, the number of cycles and the axial strain show nonlinear variation characteristics fitting a quadratic function relationship, and this fitting effect does not have a notable pattern with the change in the confining pressure. In contrast, the fitting effect gradually tends to be optimized with the increase in the unloading level. Therefore, the energy distributions at different confining pressures under 75% unloading level are provided in Table 2.

As summarized in Table 2, under the same confining pressure, only the elastic energy is positively correlated with the number of cycles, whereas the input and dissipation energies are negatively correlated. In the first cycle, the input and dissipation energies are significantly large. After entering the second cycle, the input and dissipation energies tend to gradually stabilize, whereas the elastic energy is lesser affected by the number of cycles, maintaining a small and stable growth. The analysis shows that during the first cycle of different cycle levels, the pores and fissures inside the rock are compacted and tightened, whereas the microcracks are extended and penetrated. These lengthen the compression path of the testing machine and increase the deformation of the rock; therefore, both the work done by the testing machine on the rock and input energy of the rock increase. After entering the second cycle, the compression and expansion paths shorten, and the energy consumed in producing a new plastic zone gradually decreases. The fatigue damage of the rock gradually accumulates, reducing the input and dissipation energies. Between them, the decrease in the input energy is relatively smaller than that in the dissipation energy; therefore, the elastic energy is positively correlated with the number of cycles. In addition, from Table 2, different upper stresses (of different cycle levels) also lead to differences in the energy distribution; therefore, the energy evolution laws for different cycle levels at 75% unloading level are presented in Fig. 7.

As shown in Fig. 7, the input, elastic, and dissipation energy under cyclic loading show a phase increase with the cyclic grade, i.e., the increment in each energy gradually increases with the upgrade of the cycle rank. It is inferred that under the action of a low cyclic level, the small upper limit stress causes the rock to mainly show compression closure of the internal microfractures and pores. Owing to the short compression path and cyclic load action time, the fatigue damage of the rock gradually accumulates, resulting in nonremarkable damage and gradual energy growth of the rock. With the increase in the cyclic rank, the cyclic load action time and upper limit stress increase. Therefore, the axial load on the rock under the action of a high cyclic rank lengthens the compression path and increases the compression amplitude. The phenomenon of fissure sprouting and expansion occurs inside the rock, significantly increasing the macroscopic deformation of the rock. Thus, the accumulation of fatigue damage inside the sample intensifies and the unrecoverable deformation of the rock increases, enhancing the input and dissipation energies. In addition, from Fig. 7, with the increase in the cyclic grade under the same confining pressure, the elastic energy increases more notably than the dissipation energy. Moreover, the difference between the two energies gradually increases, making the elastic energy to play

TABLE 2

Rock energy distributions at different confining pressures under 75% unloading level

Confining Pressure	Number of cycles	One-stage cycle			Two-stage cycle			Three-stage cycle			Four-stage cycle		
		Input energy	Elastic energy	Dissipation energy	Input energy	Elastic energy	Dissipation energy	Input energy	Elastic energy	Dissipation energy	Input energy	Elastic energy	Dissipation energy
		(10^{-3} MJ/m^3)			(10^{-3} MJ/m^3)			(10^{-3} MJ/m^3)			(10^{-3} MJ/m^3)		
20 MPa	1	36.69	16.2	20.49	138.19	78.19	60	372.98	207.62	165.36			
	2	24.34	16.47	7.87	102.36	78.57	23.79	276.59	210.18	66.41			
	3	23.56	16.52	7.04	100.6	78.58	22.02	274.73	212.74	61.99			
30 MPa	1	24.91	11.75	13.16	91.52	58.52	33	222.96	149.58	73.38	527.55	307.84	219.71
	2	17.1	12.07	5.03	73.75	58.71	15.04	183.41	149.82	33.59	531.86	374.16	157.7
	3	16.9	12.14	4.76	72.51	58.75	13.76	180.95	150.34	30.61	532.91	379.35	153.56
40 MPa	1	42.25	22.3	19.95	162.41	108.23	54.18	378.57	270.83	107.74	722.19	516.99	205.2
	2	30.89	22.71	8.18	134.54	108.99	25.55	326.71	270.47	56.24	634.42	525.47	108.95
	3	30.31	22.99	7.32	133.84	109.04	24.8	319.33	271.35	47.98	633.39	529.78	103.61

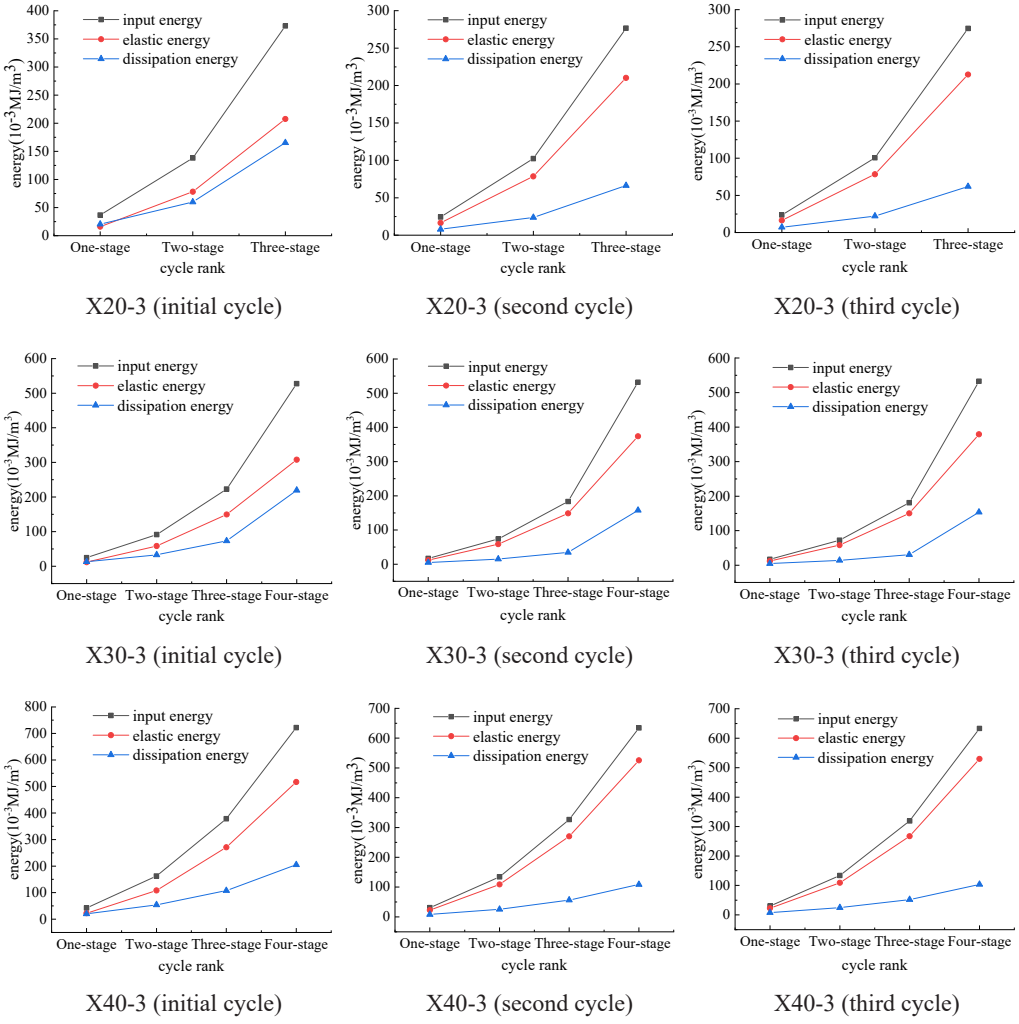

Fig. 7. Energy evolution patterns at different cycle levels under 75% unloading level

the dominant role progressively. Therefore, in order to further explore the relationship between elastic energy and dissipative energy, Fig. 8 shows the elastic and dissipated energy proportions at different envelope pressures for further comparative analysis.

From Fig. 8, it is noticeable that the elastic energy dominates the dissipation energy. Only in the first cycle, the elastic and dissipation energies are similar. With the increase in the number of cycles, the dominance of the elastic energy becomes gradually notable. This suggests that before the rock failure, the first cycle has a greater destructive effect on the rock, and the energy loss of the rock is larger, reducing the stored elastic energy. After entering the second cycle, the cyclic load causes stable damage, and the input energy during the cyclic load is mainly stored in the rock in the form of elastic energy. Only a small part of the input energy is released in the form

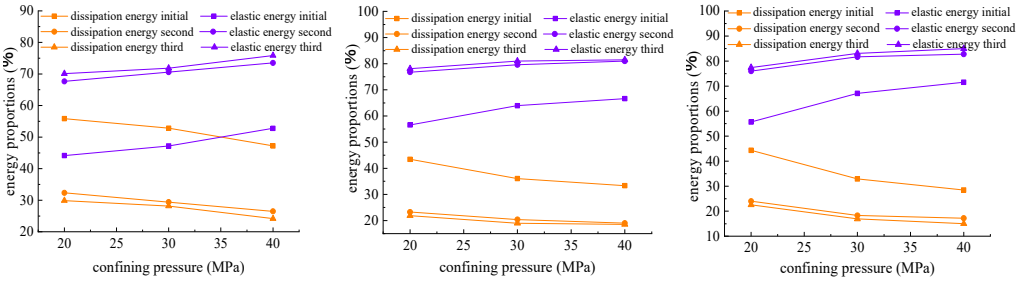

Fig. 8. Elastic and dissipated energy proportions at different envelope pressures

of dissipation energy, which significantly increases the dominant role of the elastic energy with the number of cycles. The ratio of the elastic energy to the dissipation energy is also significantly affected by the confining pressure. The ratio of the elastic energy to the surrounding pressure is positively correlated at the same cycle level, i.e., the dominance of the elastic energy in rock tends to be significant with the increase in the confining pressure. Specifically, a high confining pressure implies a strong binding effect on the rock mass and closeness of the arrangement of the internal particles of the rock. The increased resistance of the rock to deformation improves the efficiency of energy absorption and storage, and thereby enhances the limit of energy storage in the rock. A high confining pressure implies a significant binding effect, which, in turn, reduces the dissipation energy of the rock and increases the dominance of the elastic energy. The instantaneous release of elastic energy causes rock instability and failure, and the large accumulation of elastic energy creates conditions for the occurrence of floor accidents. Therefore, the greater the buried depth of coal seam, the greater the possibility and intensity of floor accidents. Fig. 9 further explores the energy evolution during cyclic addition and removal as exemplified by the X40-3 four-stage cycle.

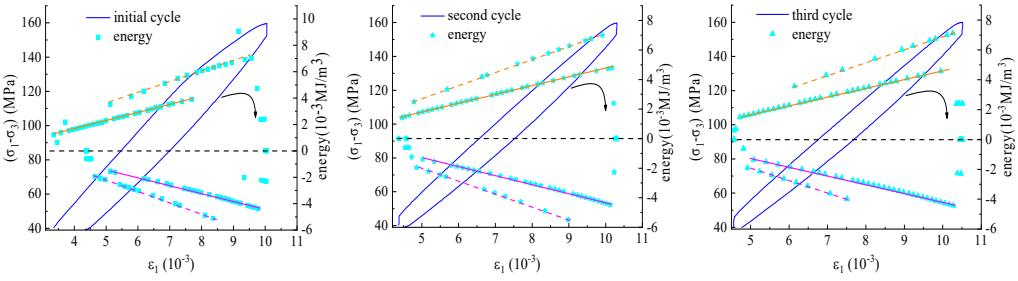

Fig. 9. Energy evolution during loading and unloading

Fig. 9 shows the stress-strain curve under different cycles. The points represent the corresponding energy values during the cycle. The input energy takes a positive value, while the elastic energy takes a negative value. The size can be quantitatively characterized by the absolute value, and the straight line is the linear fitting of the energy evolution relationship. As shown in Fig. 9, the input energy of the rock increases approximately linearly with the increase in the

axial load, and an abrupt decrease in the input energy occurs with the increase in the number of cycles. This abrupt decrease is mainly concentrated near the upper limit stress region and is approximately linearly distributed. The elastic energy has a similar evolution pattern to the input energy, with the only difference being the abrupt change in the elastic energy being concentrated near the lower limit stress. The analysis suggests that during the initial cycle, with the gradual increase in the axial load, the internal structure of the rock is damaged by compression. Moreover, a large stress implies high probability of the occurrence of the phenomenon of fracture sprouting and expansion, which increases the irreversible deformation of the rock. Moreover, maintaining stable changes in the energy is difficult, resulting in the concentration of the input energy abrupt change near the upper stress.

3.3. Basis for Determination of Rock Instability

In [34,47-48], the ratio of the dissipation energy to the elastic energy of a loaded rock was used to characterize its internal damage accumulation. A large ratio implies considerable damage accumulation inside the rock, indirectly reflecting the relative stability state of the loaded rock sample, which is used as the basis for rock instability determination. Because of the existence of primary microfractures and pores inside a rock, the process of compression and closure of the rock microfractures and fractures requires a large energy in the initial pressure density stage, dissipating remarkably more energy. With increased work done by the testing machine on the rock, the input energy of the rock increases significantly. However, the difference between the input and dissipation energies (elastic energy) does not significantly change, which increases the ratio of the dissipation energy to the elastic energy. Therefore, this ratio is used as the basis of rock instability, which is easily disturbed by the effects of rock compression in that stage. The ratio of the dissipation energy to the input energy (hereinafter referred as the energy consumption ratio) can, to a certain extent, reflect the internal damage development and plastic deformation of a rock under a certain stress level [25]. In accordance, this paper proposes to use the energy dissipation ratio to quantitatively characterize the internal damage accumulation of loaded rock samples and use it as the basis to evaluate rock instability. The energy versus ratio curves at different cycle levels and cycle times are shown in Fig. 10.

As shown in Fig. 10, the energy consumption ratio is significantly large in the first cycle and it starts to gradually decrease after entering the second cycle. The evolution of the en-

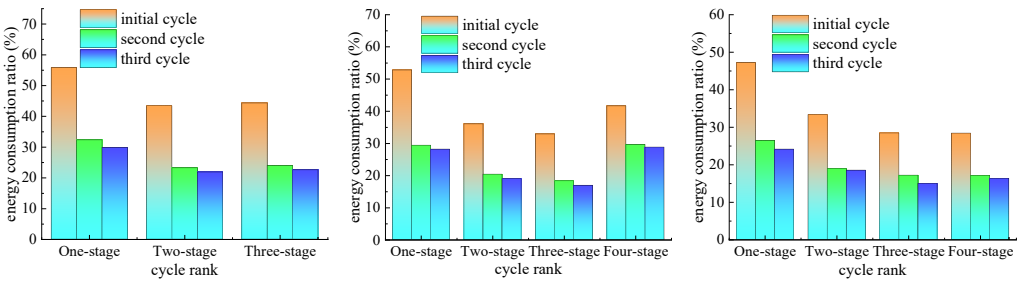

Fig. 10. Energy consumption ratios at different cycle levels and number of cycles

ergy consumption ratio is consistent under different cycle levels, indicating that the first cycle dominates rock failure, whereas the damage gradually stabilizes subsequently. During the first cycle, the energy consumption is significantly large, which is caused by the small upper stress corresponding to the compact stage of the rock. Consequently, the compacting process of the microfractures and pores inside the rock needs to consume considerable energy. Under the same unloading level, the energy consumption ratio shows different phase change characteristics with the cycle rank. With the increase in the cycle level, the energy consumption ratio shows a rapid decreasing-gradual increasing trend under the X20-3 condition, whereas it shows a rapid decreasing-gradual decreasing-rapidly increasing trend under the X30-3 condition. Under the X40-3 condition, the energy consumption ratio shows an increasing trend from a rapid declining to a gradual decreasing trend. The analysis concludes that from the initial to the second cycle, the energy consumption ratios under the X20-3, X30-3, and X40-3 conditions significantly decrease. This indicates that the rock is being further compacted or accompanied with a small amount of fracture development and expansion process with a relatively small energy loss as shown by the reduced proportion of the dissipation energy. Owing to the high energy storage capacity and accumulated elastic energy, the rock in this process is mainly characterized by elastic deformation. From the second to the third cycle, the energy consumption ratio tends to be stable under the X20-3 condition, indicating that the internal cracks of the rock expand stably in this process. Consequently, the energies consumed and absorbed tend to be stable. The energy consumption ratio steadily decreases under the X30-3 and X40-3 conditions, and the decrease under the latter is more remarkable than that under the former condition. This is attributed to the higher confining pressure leading to a higher bearing capacity of the rock. Under the confining pressure of 40 MPa, the upper limit stress of the three-stage cycle can damage the rock. Owing to the small degree of damage, cracks gradually develop or rarely evolve; therefore, the rock integrity is relatively good. Because the development and expansion of cracks require a small amount of energy, the energy consumption ratio significantly decreases. From the third to the fourth stage, the energy consumption ratio significantly increases under the X30-3 condition, indicating that the upper limit stress of the three-stage cycle is close to the peak strength. Moreover, the cracks enter the stage of rapid expansion, which promotes the formation of macroscopic fracture surfaces. The energy demand and the consumption ratio significantly increase. However, the energy consumption ratio stabilizes under the X40-3 condition, indicating that the rock is influenced by the strong binding effect of the confining pressure; only then the internal cracks start to develop and steadily expand. The energy consumption ratio evolution process can reflect well the internal damage accumulation process, and hence, characterize the destabilization and failure process of the rock. In addition, the acoustic emission monitoring system is also an important method for monitoring rock movement and deformation. Moreover, it can be used to characterize the failure process of rock failure [49-52]. Ultrasonic testing technology has been widely recognized in the field of geotechnical engineering. Therefore, the author believes that, in the future, based on the stress–strain process, the wave velocity test and energy dissipation analysis will be used to study rock masses. We shall elaborate on this in another article.

In summary, the evolution of the energy consumption ratio can be divided into three stages: rapid decreasing, stable developing, and rapid increasing stages. Among them, the stable developing stage of the energy consumption ratio can be subdivided into gradual decreasing and gradual increasing stages. The rapid increase in the energy consumption ratio mainly corresponds to the stage of rapid crack development, and a large increase in the dissipation energy implies significant damage to the rock.

4. Conclusion

(1) The rock stress-strain curve hysteresis phenomenon is remarkable under cyclic loading, with the hysteresis loop shifting in the direction of the increasing strain. Moreover, as the upper limit stress increases, the hysteresis loop tends to be 'sparse', and the hysteresis loop area gradually increases. The accumulation of fatigue damage in the specimen increases, and the residual deformation of the rock increases. The fatigue damage caused by cyclic loading has a certain weakening effect on the peak strength of the rock. Both the number of cycles and the axial strain show nonlinear variation characteristics that satisfy the quadratic function relationship. Furthermore, the stress level of the rock is the main reason affecting the fitting effect.

(2) Under the same confining pressure, with an increase in cycle level, the macroscopic deformation of rock increases, and the growth of input energy and dissipation energy increases. In the first cycle, the input energy and dissipation energy are larger, which plays a major role in the destruction of the rock. In the second cycle, the dissipation energy of rock gradually tends to stabilize, which plays a stable role in the destruction of rock. The elastic energy is affected less by the number of cycles, and maintains a slight steady growth state. The input energy is mainly stored in the rock in the form of elastic energy.

(3) In terms of elastic energy and dissipation energy, elastic energy is dominant After the second cycle, only a small part of the input energy is released in the form of dissipative energy, and the dominant position of elastic energy is gradually strengthened. In addition, confining pressure can effectively improve the efficiency of rock absorption and energy storage, enhance the energy storage limit of rock, and limit the dissipation and release of partial energy of rock. The larger the confining pressure, the more obvious the limiting effect, and the more significant the dominant position of elastic energy. Moreover, the large accumulation of elastic energy creates conditions for the occurrence of floor accidents.

(4) The evolution process of the energy dissipation ratio can reflect the internal damage accumulation process of rock well. Therefore, it can be used as the basis for judging the instability of rock and can also characterize the gradual process of floor deformation and failure. Under the same unloading level, the energy dissipation ratio is negatively correlated with the confining pressure, that is, the larger the confining pressure, the smaller the energy dissipation ratio, and the slower the accumulation of rock damage. The change in the energy dissipation ratio can be summarized into three stages: the rapid decline stage of energy dissipation ratio, the stable development stage, and the rapid rise stage. Among them, the stable development stage of the energy dissipation ratio can be divided into the slow decline and slow rise stages of the energy dissipation ratio. Among them, the greater the increase in dissipation energy, the greater the degree of rock damage.

Acknowledgments

This research was supported by the National Key Research and Development Program Sub-Task (Grant No. 2018YFC0604702), National Natural Science Foundation of China (Grant No. 51379119) and Natural Science Foundation of Shandong Province (Grant No. ZR2021ME086)
Thank you for the conditions provided by Professor Zhang and the help provided by our research team.

References

[1] H.P. Xie, Research review of the state key research development program of China: Deep rock mechanics and mining theory. Journal of China Coal Society **44** (05), 1283-1305 (2019). DOI: https://doi.org/10.13225/j.cnki.jccs. 2019.6038

[2] H.P. Xie, F. Gao, Y. Ju, M.Z. Gao, R. Zhang, Y.N. Gao, J.F. Liu, L.Z. Xie, Quantitative definition and investigation of deep mining. Journal of China Coal Society **40** (01), 1-10 (2015). DOI: https://doi.org/10.13225/j.cnki.jccs.2014.1690

[3] M.C. He, H.P. Xie, S.P. Peng, Y.D. Jiang, Study on rock mechanics in deep mining engineering. Chinese Journal of Rock Mechanics and Engineering **24** (16), 2803-2813 (2005).

[4] Y. Zhao, H.W. Zhou, W.G. Ren, J.C. Zhong, D. Liu, Permeability evolution of roof sandstone at deep coal seam working face under cyclic loading. Journal of China Coal Society **44** (05), 1495-15 (2019). DOI: https://doi.org/10.13225/j.cnki.jccs.2019.6005

[5] J.W. Zhang, W.B. Fan, W.M. Niu, S.Y. Wang, Energy evolution characteristics of deep sandstone with different true triaxial stress paths. Geomechanics and Geophysics for Geo-Energy and Geo-Resources **8** (2), 62 (2022). DOI: https://doi.org/10.1007/s40948-022-00374-6

[6] H. Wagner, Deep Mining: A Rock Engineering Challenge. Rock Mechanics and Rock Engineering **52** (5), 1417-1446 (2019). DOI: https://doi.org/10.1007/s00603-019-01799-4

[7] H.P. Song, Z, Hao. D.H. Fu, Q. Zhang, Experimental analysis and characterization of damage evolution in rock under cyclic loading. Inter-national Journal of Rock Mechanics & Mining Sciences **88**, 157-164 (2016). DOI: https://doi.org/10.1016/j.ijrmms.2016.07.015

[8] H.P. Xie, C.B. Li, M.Z. Gao, R. Zhang, F. Gao, J.B. Zhu, Conceptualization and preliminary research on deep in situ rock mechanics. Chinese Journal of Rock Mechanics and Engineering **40** (02), 217-232 (2021). DOI: https://doi.org/10.13722/j.cnki.jrme.2020.0317

[9] H.P. Xie, R.D. Peng, Y. Ju, H.W. Zhou, On energy analysis of rock failure. Chinese Journal of Rock Mechanics and Engineering **15**, 2603-2608 (2005).

[10] Y.F. Wang, F. Cui, Energy evolution mechanism in process of Sandstone failure and energy strength criterion. Journal of Applied Geophysics **154**, 21-28(2018). DOI: https://doi.org/10.1016/j.jappgeo.2018.04.025

[11] M. Hasan, Y.J. Shang, P. Shao, X.T. Yi, H. Meng, Evaluation of Engineering Rock Mass Quality via Integration Between Geophysical and Rock Mechanical Parameters. Rock Mechanics and Rock Engineering **55** (4), 2183-2203 (2022). DOI: https://doi.org/10.1007/s00603-021-02766-8

[12] H.R Renani, M. Cai, Forty-Year Review of the Hoek-Brown Failure Criterion for Jointed Rock Masses. Rock Mechanics and Rock Engineering **55** (1), 439-461 (2021). DOI: https://doi.org/10.1007/s00603-021-02661-2

[13] H.K. Yoon, J.S. Lee, J.D. Yu, Correlation of granite rock properties with longitudinal wave velocity in rock bolt. International Journal of Rock Mechanics and Mining Sciences **15** (2022). DOI: https://doi.org/10.1016/j.ijrmms.2022.105200

[14] L.T. Dvornikov, V.A. Korneyev, Design of a device for rocks strength properties determining to solve the tasks of rock rock-cutting machines design. International Conference on Modern Trends in Manufacturing Technologies and Equipment (ICMTMTE) – Materials Science 224, DOI: https://doi.org/10.1051/matecconf/201822402084

[15] M. Xu, X.U. Zhang, L. Luo, X.U. Zhao, Research on Mechanical Properties and Energy Evolution of Sandstone Under Cyclic Loading Mode. Mining Research and Development **41** (07), 123-128 (2021). DOI: https://doi.org/10.13827/j.cnki.kyyk.2021.07.023

[16] Y.N. Sun, P.S. Zhang, W. Yan, F.Q. Yan, J.D. Wu, Compressive Deformation Characteristics of Crushed Sandstone Based on Multiple Experimental Factors. Archives of Mining Sciences **65** (1), 129-146 (2020). DOI: https://doi.org/10.24425/ams.2020.132711

[17] S.J. Miao, H. Wang, Z.J. Huang, M.C. Liang, Experimental study on the mechanical properties of argillaceous quartz siltstone under different upper limit cyclic loadings. Engineering Mechanics **38** (07), 75-85 (2021).

[18] X.W. Li, Z.S. Yao, X.W. Huang, Z.X. Liu, X. Zhao, K.H. Mu, Investigation of deformation and failure characteristics and energy evolution of sandstone under cyclic loading and unloading. Rock and Soil Mechanics **42** (06), 1693-1704 (2021). DOI: https://doi.org/10.16285/j.rsm.2020.1463

[19] H.F. Deng, Y. Hu, J.L. Li, Z. Wang, X.J. Zhang, A.L. Hu, The evolution of sandstone energy dissipation under cyclic loading and unloading. Chinese Journal of Rock Mechanics and Engineering **35** (S1), 2869-2875 (2016). DOI: https://doi.org/10.13722/j.cnki.jrme.2015.0278

[20] J.W. Zhou, X.G. Yang, W.X. Fu, J. Xu, H.T. Li, H.W. Zhou, J.F. Liu, Experimental test and fracture damage mechanical characteristics of brittle rock under uniaxial cyclic loading and unloading conditions. Chinese Journal of Rock Mechanics and Engineering **29** (06), 1172-1183 (2010).

[21] H. Wang, T.H. Yang, H.L. Liu, Y.C. Zhao, W.X. Deng, X.G. Hou, Mechanical properties and energy evolution of dry and saturated sandstones under cyclic loading. Rock and Soil Mechanic **38** (06), 1600-1608 (2017). DOI: https://doi.org/10.16285/j.rsm.2017.06.008

[22] Y. Xu, C.J. Li, Q.Q. Zheng, X. Ni, Q.Q. Wang, Analysis of energy evolution and damage characteristics of mudstone under cyclic loading and unloading. Chinese Journal of Rock Mechanics and Engineering **38** (10), 2084-2091 (2019). DOI: https://doi.org/10.13722/j.cnki.jrme.2019.0153

[23] J. Yu, W. Yao, W.B. Ren, Z.Z. Fan, Deformation law of cyclic disturbance and a failure precursor feature of marble under high stress. Chinese Journal of Geotechnical Engineering 1-7.
DOI: http://kns.cnki.net/kcms/detail/32.1124.tu.20220301.0915.004.html

[24] S.G. Li, S.B. Liu, H.F. Lin, H.Q. Shuang, L.M. Li, H.X. Yu, R.W. Luo, Experimental research on deformation and failure characteristics of coal by staged cyclic loading and unloading. Coal Science and Technology **49** (04), 199-205 (2021). DOI: https://doi.org/10.13199/j.cnki.cst.2021.04.024

[25] Z.Y. Liu, X. Dong, X.Y. Zhang, Experimental study on mechanical properties of bedding coal and rock under graded cyclic loading. Chinese Journal of Rock Mechanics and Engineering **40** (S1), 2593-2602 (2021). DOI: https://doi.org/10.13722/j.cnki.jrme.2020.0643

[26] F.K. Xiao, Z.L. Shen, G. Liu, Z. Zhang, F.R. Zhang, Relationship between hysteresis loop and elastoplastic strain energy during cyclic loading and unloading. Chinese Journal of Rock Mechanics and Engineering **33** (9), 1791-1797 (2014). DOI: https://doi.org/10.13722/j.cnki.jrme.2014.09.008

[27] V. Srinivasan, T. Gupta, T.A. Ansari, T.N. Singh, An experimental study on rock damage and its influence in rock stress memory in a metamorphic rock. Bulletin of Engineering Geology and the Environment **79** (8), 4335-4348 (2020). DOI: https://doi.org/10.1007/s10064-020-01813-y

[28] X.B. Yang, H.M. Cheng, J.Q. Lü, X. Hou, C.G. Nie, Energy consumption ratio evolution law of sandstones under triaxial cyclic loading. Rock and Soil Mechanics **40** (10), 3751-3757+3766 (2019).
DOI: https://doi.org/10.16285/j.rsm.2018.2166

[29] Q.L. Li, Z.J. Jia, H.L. Fu, Experimental study on dynamic characteristics of sandstone under cyclic loading and different confining pressures. Journal of Railway Science and Engineering **16** (10), 2459-2466 (2019).
DOI: https://doi.org/10.19713/j.cnki.43-1423/u.2019.10.011

[30] Z.W. Ni, X.G. Wu, H. Chen, Y.X. Zhou, Study on Mechanical Properties of Sandstone under Grading Cyclic Loading and Unloading Test. Metal Mine (10), 21-27 (2021). DOI: https://doi.org/10.19614/j.cnki.jsks. 202110004

[31] G.J. Cai, W.P. Sun, X.R. Chen, S.L. Yang, J. Jia, L. Li, Study on the damage mechanical properties of sandstone under cyclic loading and unloading in stages. China Measurement & Test 1-7.
DOI: http://kns.cnki.net/kcms/detail/51.1714.TB.20220322.1747.024.html

[32] R.H. Wang, Y.Z. Jiang, J. Liu, Y. Wang, Experimental Study of Deformation Characteristics of Sandstone Under Cyclic Loading and Unloading Conditions. Journal of Mining & Safety Engineering **28** (02), 231-235 (2011).

[33] Y. Zhang, J. Xu, H.W. Yang, J.N. Wang, Effect of confining pressure on evolution law of hysteresis loop of sandstone under cyclic loading. Chinese Journal of Rock Mechanics and Engineering **30** (02), 320-326 (2011).

[34] Q.B. Meng, C.K. Wang, B.X. Huang, H. Pu, Z.Z. Zhang, W. Sun, J. Wang, Rock energy evolution and distribution law under triaxial cyclic loading and unloading conditions. Chinese Journal of Rock Mechanics and Engineering **39** (10), 2047-2059 (2020). DOI: https://doi.org/10.13722/j.cnki.jrme.2020.0208

[35] S.S. Zhang, E.L. Liu, J.H. Zhang, Experimental study of fatigue damage properties of sandstone samples under cyclic loading with low frequencies. Chinese Journal of Rock Mechanics and Engineering **33** (S1), 3212-3218 (2014). DOI: https://doi.org/10.13722/j.cnki.jrme.2014.s1.087

[36] R.D. Peng, Y. Ju, F. Gao, H.P. Xie, P. Wang, Energy analysis on damage of coal under cyclical triaxial loading and unloading conditions. Journal of China Coal Society **39** (02), 245-252 (2014).
DOI: https://doi.org/10.13225/j.cnki.jccs.2013.2010

[37] P. Jia, N. Yang, D.Q. Liu, D.C. Wang, S.H. Wang, Y. Zhao, X.T. Xu, Failure mechanism of combined rock under true triaxial loading and unloading conditions. Journal of Central South University(Science and Technology) **52** (08), 2867-2875 (2021).

[38] J.X. Yang, M.K. Luo, X.W. Zhang, N. Huang, S.J. Hou, Mechanical properties and fatigue damage evolution of granite under cyclic loading and unloading conditions. Journal of Mining and Strata Control Engineering **3** (03), 91-98 (2021). DOI: https://doi.org/10.13532/j.jmsce.cn10-1638/td.20210510.001

[39] J. Zhao, G.T. Guo, D.P. Xu, X. Huang, C. Hu, Y.L. Xia, D. Zhang, Experimental study of deformation and failure characteristics of deeply-buried hard rock under triaxial and cyclic loading and unloading stress paths. Rock and Soil Mechanics **41** (05), 1521-1530 (2020). DOI: https://doi.org/10.16285/j.rsm.2019.1604

[40] T.R. Stacey, J. Wesseloo, Design and Prediction in Rock Engineering: The Importance of Mechanisms of Failure, with Focus on High Stress, Brittle Rock Conditions **55** (3), 1517-1535 (2022). DOI: https://doi.org/10.1007/s00603-021-02721-7

[41] P.S. Zhang, D.Q. Xu, R. Zhang, X.L. Zhang, Y.H. Dong, W.L. Mu, Experimental study on seepage and mechanical properties of sandstone under different confining pressures and cyclic loads. Chinese Journal of Rock Mechanics and Engineering **41** (12): 2432-2450 (2022). DOI: https://doi.org/10.13722/j.cnki.jrme.2022.0241

[42] The National Standards Compilation Group of Peoples Republic of China. GB/T50266 – 99Standard for tests method of engineering rock masses. Beijing: China Planning Press (1999).

[43] D. Head, T. Vanorio, Effects of changes in rock microstructures on permeability: 3-D printing investigation. Geophysical Research Lettersb **43** (14), 7494-7502 (2016). DOI: https://doi.org/10.1002/2016GL069334

[44] Y.P. Chen, D.Y. Xi, Y.W. Xue, Dynamic stress-strain response of saturated rock under cyclic loading. Oil Geophysical Prospectingv (04), 409-413, 462-9 (2003).

[45] X Li, P.C. Zhang, Mechanical Characteristics and Energy Evolution Law of Yellow Sandstone under Cyclic Loading and Unloading Test. Journal of Yangtze River Scientific Research **38** (04), 124-131 (2021).

[46] Y.S. Xie, M. Ji, Y. Xu, Mechanics of mine rock mass. Xuzhou: China University of Mining and Technology Press (2016).

[47] D. Huang, Q. Tan, R.Q. Huang, Mechanism of strain energy conversion process for marble damage and fracture under high stress and rapid unloading. Chinese Journal of Rock Mechanics and Engineering **31** (12), 2483-2493 (2012).

[48] Z.Y. Li, G. Wu, T.Z. Huang, Y. Liu, Variation of energy and criteria for strength failure of shale under traixial cyclic loading. Chinese Journal of Rock Mechanics and Engineering **37** (3), 662-670 (2018). DOI: https://doi.org/10.13722/j.cnki.jrme.2017.0927

[49] L.J. Dong, Z.W. Pei, X. Xie, Y.H. Zhang, X.H. Yan, Early identification of abnormal regions in rock-mass using travel time tomography. Engineering (2022). DOI: https://doi.org/10.1016/j.eng.2022.05.016

[50] L.J. Dong, X.J. Tong, J. Ma, Quantitative Investigation of Tomographic Effects in Abnormal Regions of Complex Structures. Engineering **7** (7), 1011-1022 (2021). DOI: https://doi.org/10.1016/j.eng.2020.06.021

[51] T.M. He, Q. Zhao, J. Ha, K.W. Xia, G. Grasselli, Understanding progressive rock failure and associated seismicity using ultrasonic tomography and numerical simulation. Tunnelling and Underground Space Technology **81**, 26-34 (2018). DOI: https://doi.org/10.1016/j.tust.2018.06.022

[52] L.J. Dong, Q. Tao, Q.C. Hu, Influence of temperature on acoustic emission source location accuracy in underground structure. Transactions of Nonferrous Metals Society of China **31** (8), 2468-2478 (2021). DOI: https://doi.org/10.1016/S1003-6326(21)65667-4